Supplement of Geosci. Instrum. Method. Data Syst., 11, 93–109, 2022
https://doi.org/10.5194/gi-11-93-2022-supplement

Geoscientific Instrumentation Methods and Data Systems
Open Access
EGU

Supplement of

Towards agricultural soil carbon monitoring, reporting, and verification through the Field Observatory Network (FiON)

Olli Nevalainen et al.

Correspondence to: Olli Nevalainen (olli.nevalainen@fmi.fi)

S1 Calibration protocol details

The parameters of the BASGRA_N model (https://github.com/PecanProject/pecan/tree/v1.7.2/models/basgra/src) were screened with a global sensitivity analysis by varying the parameter values in their prior range. Priors are probability distributions encapsulating the likely values of model parameters that are formulated according to information coming from previous analyses, the literature, meta analyses, expert opinion, ecological theory etc. In this study, priors are chosen according to values provided by model developers and our expert opinion (also see Höglind et al., 2016; Hjelkrem et al., 2017, Huang et al., 2021). The top 20 parameters (see Table S1.1 below) that contribute most to model net ecosystem exchange (NEE) and leaf area index (LAI) output uncertainties were chosen for targeting in the calibration. Both the modeling and calibration approaches as implemented in PEcAn software are transparent, scalable and state-of-the-art techniques (Fer et al., 2018; 2021). Calibration is done by assimilating both the LAI and NEE data streams simultaneously. The influence of NEE time-series were corrected for effective sample size as described in Fer et al. (2018). Due to the coarser time step and smaller sample size of the LAI data, no additional autocorrelations were applied for this data stream.

Table 1. BASGRA Parameters targeted in the calibration.

BASGRA parameter	Description	Unit	Prior	Posterior
RUBISC	Rubisco content of upper leaves	g m-2 leaf	Unif[3,12]	Lnorm[1.5, 0.24]
LAICR	LAI above which shading induces leaf senescence	m2 leaf m-2	Unif[2, 7]	Lnorm[0.87, 0.25]
Dparam	Constant in the calculation of dehardening rate	°C-1 d-1	Unif[0.0005, 0.0018]	Norm[0.002, 0.0004]
KRESPHARD	Carbohydrate requirement of hardening	g C g-1 C °C-1	Lnorm[-3.39, 0.22]	Lnorm[-3.5, 0.2]
NCSHMAX	Maximum N-C ratio of shoot	g N g-1 C	Unif[0.015, 0.06]	Weibull[3.5, 0.04]
TCSOMF	Time constant of fast SOM decomposition at 10°C	d	Gamma[130, 0.055]	Lnorm[7.8, 0.07]
TMAXF	Temperature at which decomposition is maximal	°C	Weibull[26, 53]	Weibull[30.5, 53.02]
TSIGMAF	Resilience of decomposition to temperature change	°C	Gamma[100, 4.5]	Gamma[252, 12]
LAIEFT	Decrease in tillering with leaf area index	m2 leaf m-2	Unif[0.01, 0.4]	Weibull[4, 0.3]
NELLVM	Number of elongating leaves per non-elongating tiller	tiller-1	Unif[1, 3]	Weibull[5.54, 2.42]
RDRSCO	Relative death rate of leaves and non-elongating tillers	d-1	Unif[0.03, 0.13]	Weibull[5.85, 0.1]

LAITIL	Maximum ratio of tiller and leaf appearance at low leaf area index	-	Unif[0.3, 1.2]	Gamma[31, 66.8]
RDRTMIN	Minimum relative death rate of foliage	d-1	Beta[20, 1250]	Beta[66.3, 3403]
TCNUPT	Time constant of soil mineral N uptake	d	Unif[10, 70]	Weibull[2.55, 42]
K	PAR extinction coefficient	m2 leaf m-2	Unif[0.5, 0.95]	Norm[0.7, 0.1]
FLITTSOMF	Fraction of decomposed litter becoming fast SOM	g g-1	Beta[170, 80]	Beta[245.8, 112.4]
TBASE	Minimum value of effective temperature for leaf elongation	℃	Unif[0.1, 6]	Weibull[1.76, 1.81]
TRANCO	Transpiration coefficient	mm d-1	Lnorm[1.5, 0.45]	Lnorm[1.4, 0.34]
SLAMAX	Maximum SLA of new leaves	m2 leaf kgC-1	Norm[40, 2]	Norm[39.3, 1.93]
FSOMFSOMS	Fraction of decomposed fast SOM	g g-1	Beta[10, 250]	Beta[16.9, 453.9]

Unif: Uniform, Norm: Normal (Gaussian), Lnorm: Log-normal

S2 Case study: To delay or not to delay harvest

The grass at the Qvidja farm had a remarkable difficulty in recovering after the first harvest on 14 June 2021) because the following days were particularly hot and dry. This resulted in poor carbon assimilation in the following weeks after the harvest (see online graphs on Field Observatory, www.fieldobservatory.org). To devise a scenario where we evaluate the impact of timing of this harvest (e.g. what if it was harvested one week later), we travel back in time to 14 June 2021 where the farmer is facing the decision whether to cut the grass today (14 June, what happened in reality) or later (e.g. 21 June, alternative scenario). We restart the model from the states as of 13 June 2021 (which we archived) and run it forward with the 15-day weather forecast drivers available to us at the time (which we also archived). In other words, we start the model from its retrospective states and we don't use the now observed weather drivers for this period but the 15-day weather forecast to mimic a real-life scenario. The available forecast horizon for the farmer in this case is the next 15 days as of 14 June (until and including 28 June).

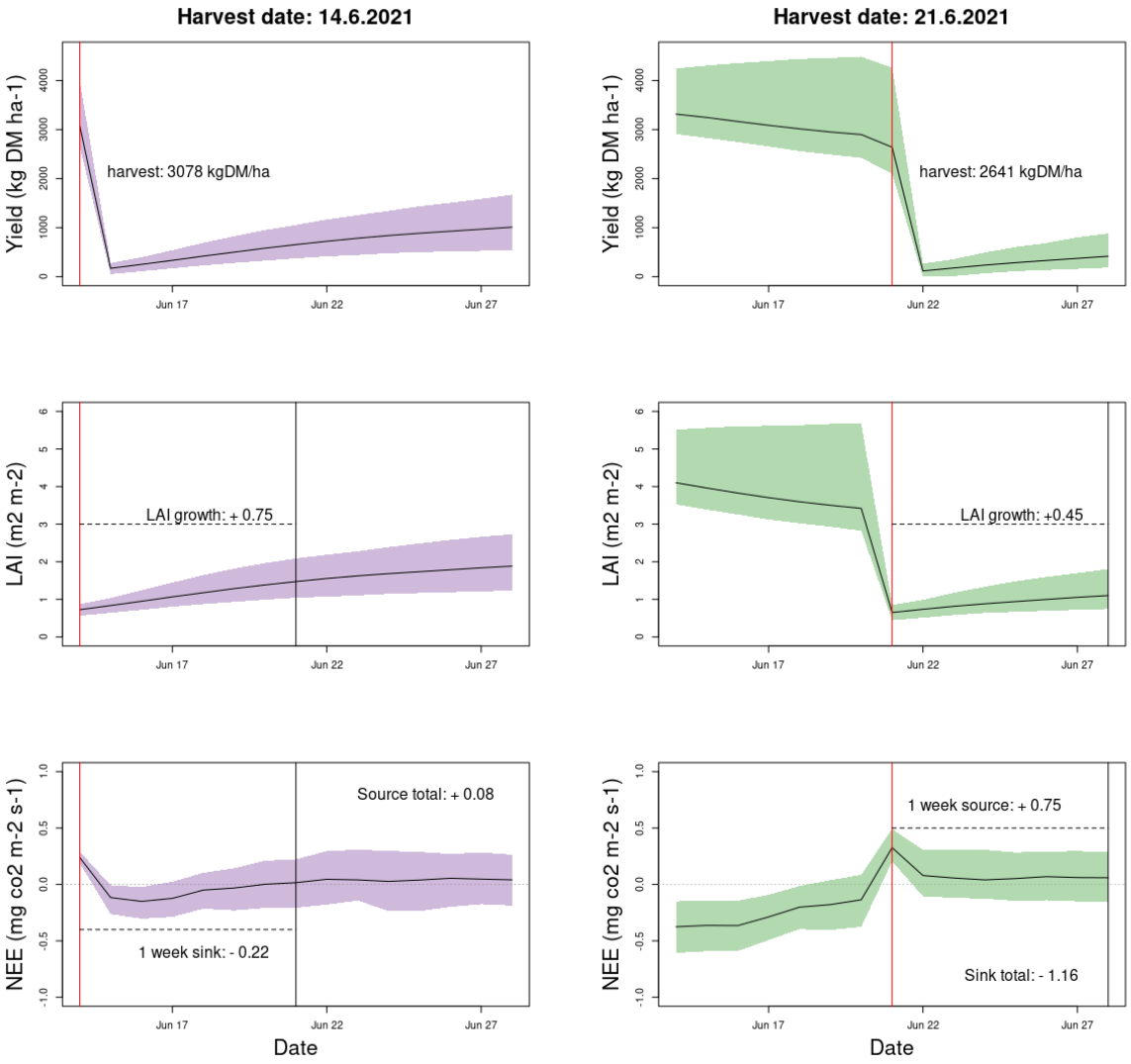

Figure S2.1 Alternative scenario of delaying (right column) the harvest date (red vertical lines) leads to a slightly larger C sink within the 15-day period while resulting in less yield. LAI stands for leaf area index and NEE for net ecosystem exchange where negative values indicate uptake and positive release of CO_2 from the ecosystem to the atmosphere.

Delaying the harvest results in ~14% less yield for the farmer (Fig S2.1, top row). Both leaf area index (LAI) development (Fig S2.1, middle row) and net ecosystem exchange (NEE; Fig S2.1, bottom row) during the week following the harvest imply that delaying the harvest may have some adverse effects compared to the real case. While leaving the grass intact longer during the 14–21 June period contributes to the overall C sink within this 2-week period (+0.08 vs alternative -1.16), it is not clear (from the perspective of carbon storage) whether the amount (even if we account for yield difference as a C

output from the system) justifies delaying harvest on the whole at the expense of yield. Looking at this picture, considering the next 15-day forecast on 14 June, the farmer could be advised to keep the harvest date as 14 June in this case study.

To observe post-hoc what will happen to the C sequestration at this period later in the season, we run the model forward until the end of our predefined growing season, 31 October and calculate the C balance over the 14 June to 31 October period. Note that this is just a forward run without being informed by the observations during this period, therefore this should be taken as a relative comparison. When we consider only the fluxes between the ecosystem and atmosphere, the actual harvest time was more favourable, i.e. it acted as a higher sink than the alternative case (-1251 kgC ha-1 vs. alternative -861 kgC ha-1, Fig. S2.2). If the carbon removed as yield is also considered, the actual harvest day was again more favourable (+288 kgC ha-1 vs. alternative +453 kgC ha-1, Fig. S2.2). This suggests that keeping the harvest time as it is might have indeed been preferred.

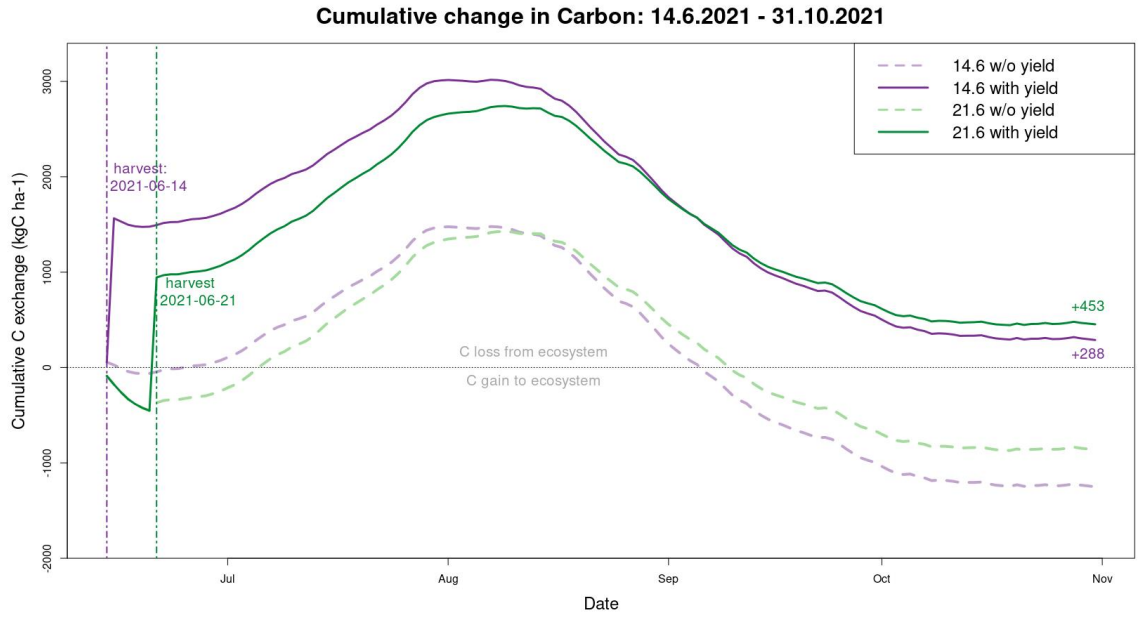

Figure S2.2 Accumulation of carbon over 14 June to 31 October period followed by the two cutting days: actual on June 14 and alternative on June 21. Positive values indicate C loss from the ecosystem, and vice versa. Dashed lines do not take into account the carbon outflow via harvest. Gain in delaying harvest date is lost later in the examined period.

While this is a demonstration, it exemplifies types of experiments that can be designed through this framework. Here we used a static and arbitrary one week delay and considered only yield, LAI and NEE variables, but more dynamic, systematic and longer-term explorations are also being devised. In addition, other constraints, such as the practical flexibility in the agricultural activities of an average farm should also be taken into account.

References

Fer, I., Kelly, R., Moorcroft, P. R., Richardson, A. D., Cowdery, E. M., and Dietze, M. C.: Linking big models to big data: efficient ecosystem model calibration through Bayesian model emulation, Biogeosciences, 15, 5801–5830, https://doi.org/10.5194/bg-15-5801-2018, 2018.

Fer, I., Gardella, A. K., Shiklomanov, A. N., Campbell, E. E., Cowdery, E. M., De Kauwe, M. G., Desai, A., Duveneck, M. J., Fisher, J. B., Haynes, K. D., Hoffman, F. M., Johnston, M. R., Kooper, R., LeBauer, D. S., Mantooth, J., Parton, W. J., Poulter, B., Quaife, T., Raiho, A., Schaefer, K., Serbin, S. P., Simkins, J., Wilcox, K. R., Viskari, T., and Dietze, M. C.: Beyond ecosystem modeling: A roadmap to community cyberinfrastructure for ecological data-model integration, Glob. Change Biol., 27, 13–26, https://doi.org/10.1111/gcb.15409, 2021.

Hjelkrem, A.-G. R., Höglind, M., van Oijen, M., Schellberg, J., Gaiser, T., and Ewert, F.: Sensitivity analysis and Bayesian calibration for testing robustness of the BASGRA model in different environments, Ecological Modelling, 359, 80–91, https://doi.org/10.1016/j.ecolmodel.2017.05.015, 2017.

Höglind, M., Van Oijen, M., Cameron, D., and Persson, T.: Process-based simulation of growth and overwintering of grassland using the BASGRA model, Ecological Modelling, 335, 1–15, https://doi.org/10.1016/j.ecolmodel.2016.04.024, 2016.

Huang, X., Zhao, G., Zorn, C., Tao, F., Ni, S., Zhang, W., Tu, T., and Höglind, M.: Grass modelling in data-limited areas by incorporating MODIS data products, Field Crops Research, 271, 108250, https://doi.org/10.1016/j.fcr.2021.108250, 2021.